PACS numbers: 42.55.Rz; 42.55.Xi; 42.79.Jq
DOI: 10.1070/QE2005v035n06ABEH003892

Highly efficient, compact diode-pumped acousto-optically *Q*-switched 1.064-μm Nd^{3+} : YAG laser operating in cw and pulsed regimes

V.V. Bezotosnyi, N.F. Glushchenko, I.D. Zalevskii, Yu.M. Popov, V.P. Semenkov, E.A. Cheshev

***Abstract*. The advantages and limitations of using highly bright laser diodes for pumping low- and moderate-power solid-state Nd^{3+} : YAG lasers are considered. The practice of designing cw and pulsed, acousto-optically *Q*-switched solid-state lasers is analysed and their possible applications are discussed. The efficiency of a cw laser achieved 50 %.**

Keywords: *solid-state laser, diode pumping*.

The use of cw laser diodes (LDs) with the output power up to a few watts for pumping solid-state lasers makes it possible to built comparatively simple and, hence, inexpensive efficient solid-state lasers, which find a variety of applications due to their compactness and high efficiency [1]. The conversion efficiency of pump radiation to the solid-state laser radiation and the total efficiency of the laser are considerably increased if pumping is produced by high-power and durable highly bright LDs (with the output power up to 4 W and the 200-μm strip contact width).

Note that pumping by high-power and high-brightness LDs produces a high thermal load on the active element of a solid-state laser, which requires a more careful consideration of the thermooptic distortions of the active medium [2]. In this paper we study the features of the laser operation in the *Q*-switching regime as compared to the cw regime upon LD pumping.

We consider the end (longitudinal) pumping of the circular active rod, which is the most efficient scheme for pumping low- and moderate-power lasers (the scheme of the pulsed laser resonator is shown in Fig. 1). The study was performed for a Nd^{3+} : YAG laser pumped to the $^4F_{5/2}$ level.

To obtain efficient lasing, the emission spectrum of a pumping LD should be exactly matched with the absorption band of the active medium, and the spatial characteristics of the pump radiation should correspond to those of the resonator mode of the solid-state laser.

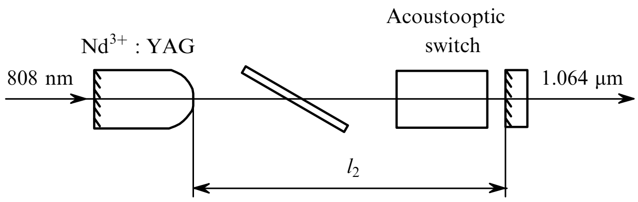

Figure 1. Scheme of the resonator of a pulsed laser (l_2 is the length of the right arm of the resonator).

The maximum of the LD emission spectrum was made coincident with the most intense 808-nm absorption band of the Nd ions by varying the LD temperature with the help of a Peltier thermoelectric module. The required accuracy of the LD temperature control (0.2 °C) was determined by the width (1 nm) of the absorption spectrum of the Nd ions and the coefficient of the temperature tuning of the emission spectrum (0.3 nm K^{-1} for AlGaAs/GaAs heterostructure lasers).

An important feature of the end pumping is a considerable longitudinal inhomogeneity of the absorbed power and, hence, of the heat release sources in the active element. In the case of cw lasers, the absorbed power is distributed along the longitudinal direction in the active element according to the Bouguer law with the absorption coefficient α. Active elements in the form of circular rods are commonly cooled on the side surface, and both the longitudinal and transverse temperature distributions appear in them upon end pumping. The temperature field in the active element in our case was described by the two-dimensional stationary heat conduction equation with the fourth-order boundary conditions on the side surface [3]. Its solution was obtained in the form of a Fourier – Bessel series.

Figure 2 shows the calculated transverse temperature distributions in the pump region ($r < 0.15$ mm) near the end and in the middle of the active element. The longitudinal temperature distribution is inhomogeneous, the active medium being strongly heated near the rod end through which pumping is performed. For the pump power of 4 W and the diameter of pump region 0.3 mm, the temperature of the active region exceeds that of the side surface by 28 K. As the pump power is increased up to 10 W, the temperature excess achieves 70 K and is accompanied by a decrease in the lasing efficiency.

V.V. Bezotosnyi, Yu.M. Popov, E.A. Cheshev P.N. Lebedev Physics Institute, Russian Academy of Sciences, Leninskii prosp. 53, 119991 Moscow, Russia; e-mail: cheshev_e2003@mail.ru;
N.F. Glushchenko Scientific-Research Institute for Precision Instrument Making, ul. Aviamotornaya 53, 111250 Moscow, Russia;
I.D. Zalevskii M.F. Stel'makh Polyus Research & Development Institute, ul. Vvedenskogo 3, 117342 Moscow, Russia;
V.P. Semenkov Ryazan State Instrument-Making Enterprise, ul. Kalyaeva 8, 390000 Ryazan, Russia

Received 22 February 2005; revision received 28 April 2005
Kvantovaya Elektronika **35** (6) 507 – 510 (2005)
Translated by M.N. Sapozhnikov

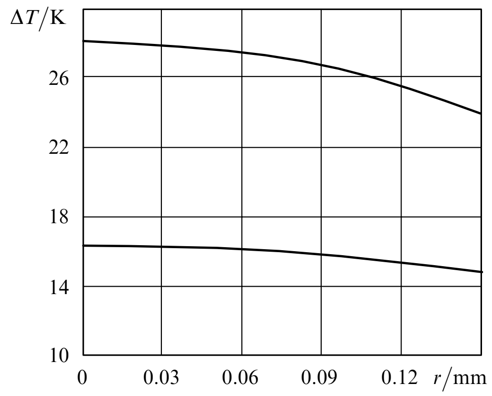

Figure 2. Transverse temperature distribution in the pump zone in two sections of the active element: on the end (upper curve) and in the middle (lower curve).

The temperature-field gradient in the transverse direction determines in turn the optical power of induced thermooptic distortions. The end pumping produces the inhomogeneous longitudinal distribution of thermooptic distortions, which is close to exponential and is located in the region $0 < z < 1/\alpha$. This allows one to calculate the resonator by replacing a distributed thermal lens by a lumped one, located at a distance of $1/\alpha$ from the rod end, with the optical power [4]

$$P_{\rm to} = \frac{1}{f_{\rm to}} = \frac{{\rm d}n}{{\rm d}T}\frac{W_{\rm p}\eta_{\rm to}}{2\pi r_{\rm p}^2\lambda},$$

where $W_{\rm p}$ is the pump power; $f_{\rm to}$ is the focal distance of a thermal lens; $\eta_{\rm to} \approx 0.24$ is the heat release coefficient; ${\rm d}n/{\rm d}T = 9\times10^{-6}$ K^{-1} is the temperature coefficient of the refractive index of the garnet [5]; $\lambda = 0.013$ W mm^{-1}K^{-1} is the heat conduction of the garnet [5]; and $r_{\rm p}$ is the pump region radius. In our case, the optical power of the thermal lens was 4.75 m^{-1} for the pump power 4 W.

We used the model of a lumped thermal lens for calculating the resonator by the methods of matrix geometrical optics. Both plane and spherical surfaces of the output mirror and active element ends were taken into account. Figure 3 shows the typical dependences of the fundamental-mode radius in the active element and on the output mirror on the length l_2 of the right arm of the resonator.

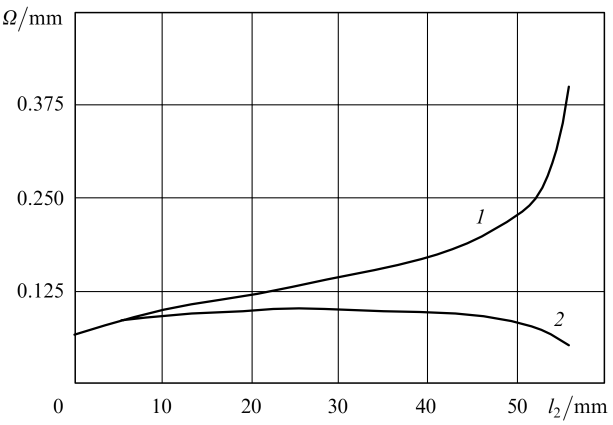

Figure 3. Dependences of the fundamental-mode radius Ω on the length l_2 of the right arm of the resonator in the active element (*1*) and on the output mirror (*2*).

We used the resonator that was close to the semiconfocal one and provided the selection of the fundamental TEM$_{00}$ mode and a high lasing efficiency along with a low sensitivity to variations in the pump power in the range 3 – 4 W. This resonator was employed in a cw laser and, with some variations in the design, in an acousto-optically *Q*-switched laser.

Although the distributions of the pump power, field temperature, and thermooptic distortions in the *Q*-switching regime become more uniform, the position of a distributed thermal lens with respect to the active element end is retained. Therefore, conclusions obtained for a cw laser are also valid for *Q*-switched lasers.

It is known [6 – 8] that the energy characteristics weakly depend on the longitudinal distribution of the pump power and can be calculated from averaged balance equations

$$\frac{{\rm d}\varDelta}{{\rm d}t} = W_{14}(n_0 - \varDelta) - J\sigma_{\rm eff}\varDelta - \frac{\varDelta}{\tau},$$

$$\frac{1}{c}\frac{{\rm d}J}{{\rm d}t} = J\sigma_{\rm eff}\varDelta - J(\beta_{\rm p} + \beta_{\rm a}),$$

which allow one to obtain the expression for the output power of a cw laser far above the threshold:

$$W_{\rm cw} = \gamma W_{\rm p}\frac{\nu_{\rm g}}{\nu_{\rm p}}\frac{\beta_{\rm a}}{\beta_{\rm a} + \beta_{\rm p}}.$$

Here, J is the average intensity of the sum of waves in the resonator; $\varDelta$ is the average inversion population; c is the speed of light in the active medium; $\sigma_{\rm eff} = 3.3\times10^{-19}$ cm^2 is the effective cross section of the lasing transition; τ is the radiative lifetime; γ is the pump efficiency (quantum yield); $\nu_{\rm g}$, $\nu_{\rm p}$ are the lasing and pump frequencies, respectively; $W_{14} = \gamma W_{\rm p}/(h\nu_{\rm p}V_{\rm p}n_0)$ is the pump rate; $V_{\rm p}$ is the volume of the active (pumped) medium; n_0 is the concentration of neodymium ions; h is the Planck constant; $\beta_{\rm a} = \ln(1/R)/2l$; $\beta_{\rm p}$ is the averaged coefficient of inactive resonator losses; l is the active element length; and R is the output mirror reflectivity (the second mirror is highly reflective). For the pump power of 4 W, the output power of a cw laser with high-quality active elements achieves 1.9 – 2 W, i.e., the conversion efficiency of pump radiation to the output of a solid-state laser can be as high as 50 %.

The averaged balance equations also well describe the main parameters of a *Q*-switched laser. Note, however, that the insertion of a *Q* switch and a polariser into the resonator of a cw laser increases the losses up to the value $\beta_{\rm p}^*$, so that the output power of the laser decreases down to $W_{\rm cw}^*$.

By solving the averaged balance equations, we can also find the average output power $W_{\rm m}$ of a repetitively pulsed laser as a function of the power of a cw laser with losses $\beta_{\rm p}^*$:

$$W_{\rm m} = \gamma^* W_{\rm cw}^*\frac{\tau_{\rm r}}{t_{\rm i}}\left[1 - \exp\left(-\frac{t_{\rm i} - t_0}{\tau_{\rm r}}\right)\right],$$

where $t_{\rm i}$ is the pulse repetition period; t_0 is the time of the *Q* switch in the open state; γ^* is the pump efficiency of the *Q*-switched laser; and $\tau_{\rm r} = \tau/(1 + \tau W_{14})$ is the pump constant.

A special feature of Q-switched lasers is a decrease in the pump efficiency with increasing population inversion, which is taken into account in the above expression with the help of the coefficient γ^*.

Figure 4 shows the dependence of the average output power of the Q-switched laser on the pulse repetition rate $F = 1/t_\mathrm{i}$, which is in good agreement with experimental data. After the insertion of a polariser and a Q switch into the resonator, the output power of the cw laser reduced by 10 % – 15 %. The average output power of the Q-switched laser achieved 1.4 – 1.5 W. Its lower value compared to the calculated 1.6 – 1.8 W is explained by the influence of neglected factors such as superluminescence and a longitudinal inhomogeneity of the pump. In addition, in the case of high pulse repetition rates, when the pulse repetition period is much shorter than the metastable-level lifetime, it is necessary to take into account an incomplete de-excitation of the active medium. This requires the use of more accurate expressions following from balance equations.

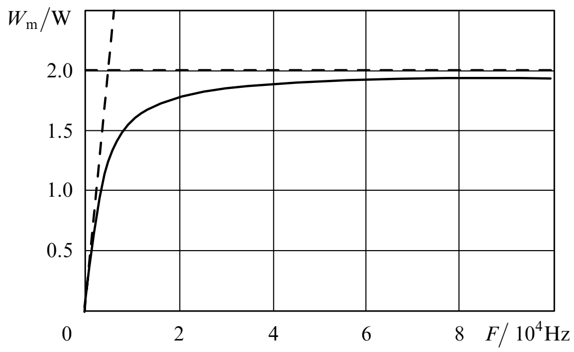

Figure 4. Dependence of the average power of the Q-switched laser on the pulse repetition rate (solid curve) and its asymptotes (dashed straight lines).

The plot of the average output power of the laser is limited by two asymptotes. For low frequencies, when $F \ll 1/\tau_\mathrm{r}$,

$$W_\mathrm{m} = W^*_\mathrm{cw}\frac{\tau_\mathrm{r}}{t_\mathrm{i}};$$

for high frequencies ($1/\tau_\mathrm{r} < F \ll 1/t_0$),

$$W_\mathrm{m} = W^*_\mathrm{cw}\left(1 - \frac{t_0}{t_\mathrm{i}}\right).$$

These dependences can be used to calculate the average power of the Q-switched laser in these ranges.

The pulse duration τ_g of a Q-switched laser is determined by the resonator length and the active medium gain. An increase in the pulse repetition rate reduces the accumulation time of the pump energy, resulting in a decrease in the gain in the active medium. Figure 5 presents the experimental dependence of the laser pulse duration on the pulse repetition rate.

These measurements showed that, despite a comparatively slow acousto-optic Q-switching (for 300 ns), the laser pulse duration can be a few nanoseconds (for a pulse repetition rate of 1 kHz and lower, $\tau_\mathrm{g} \lesssim 6.5$ ns). At higher pulse repetition rates, the pulse duration increases in fact linearly with the pulse repetition rate, achieving 140 ns for $F = 300$ kHz.

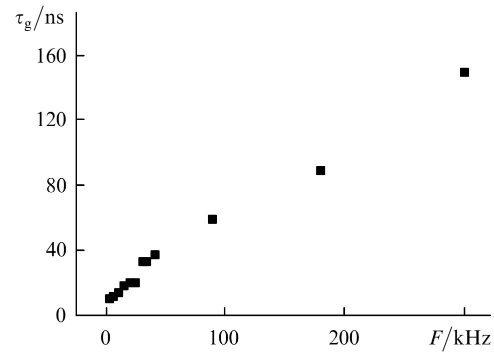

Figure 5. Dependence of the laser pulse duration on the pulse repetition rate.

The characteristics of our pulsed laser with an acousto-optic switch are presented below. The parameters of the laser in the cw regime are given in parentheses.

Radiation wavelength/μm	1.064
Mode	TEM_{00}
Beam diameter/mm	~ 0.3
Radiation divergence/mrad	less than 5.5 (less than 5)
Linear polarisation	no less than 100 : 1
Pulse repetition rate/kHz	up to 300
Pulse duration/ns	6 – 140
Output power/W	up to 1.5 (up to 1.8)
Instability (%)	1
Environment temperature/°C	10 – 40
Dimensions/mm	35 × 55 × 140
Weight/kg	0.8

The photograph of the laser head without the power supply is shown in Fig. 6.

Note in conclusion that the influence of the longitudinal inhomogeneity of the pump is mainly manifested as a displacement of 'the centre of gravity' of a thermal lens. And although we studied in this paper a neodymium-doped

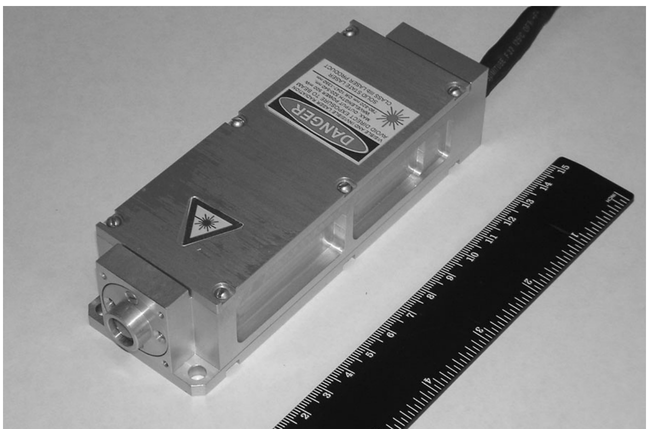

Figure 6. Laser head.

garnet, the main results, in particular, the dependence of the average power of the *Q*-switched laser on the pulse repetition rate can be also applied to other popular crystals such as Nd : YVO_4 and Nd : LSB, which have a lower heat conduction than that of the garnet and therefore require a correct consideration of effects caused by the active medium heating. The maximum output cw power was 1.8 W for the LD pump power equal to 3.6 W. Therefore, the light – light conversion efficiency was 50 %. The pulse duration was 10 ns for a pulse repetition rate of 5 kHz, the pulse energy achieving 120 μJ. The cw laser developed in this work can be used in medicine, communications, and scientific research. The pulsed laser can find applications in ranging, location, and product labelling.

Acknowledgements. This work was supported by the Russian Foundation for Basic Research (Grant No. 04-02-08251).

References

1. Byshevskaya L.O., Konopko L.O., Vorob'ev I.L., Izyneev A.A., Sadovskii P.I. *Kvantovaya Elektron.*, **34**, 809 (2004) [*Quantum Electron.*, **34**, 809 (2004)].
2. Clarkson W.A. *Proc. SPIE Int. Soc. Opt. Eng.*, **3682**, 2, (1998).
3. Tikhonov A.N., Samarskii A.A. *Uravneniya matematicheskoi fiziki* (Equations of Mathematical Physics) (Moscow: Nauka, 1977).
4. Foster J.D., Osterink L.M. *J. Appl. Phys.*, **41** (9), 3656, 1970
5. Kaminskii A.A. *Laser Crystals: Their Physics and Properties* (Berlin: Springer, 1981; Moscow: Nauka, 1975).
6. Mikaelyan A.L., Ter-Mikaelyan M.L., Turkov Yu.G. *Opticheskie generatory na tverdom tele* (Solid-state Lasers) (Moscow: Sov. Radio, 1967).
7. Stepanov B.I. (Ed.) *Metody rascheta opticheskikh kvantivykh generatorov* (Methods for Calculating Lasers) (Minsk: Institute of Physics, AN BSSR, 1966).
8. Pakhomov I.I., Rozhkov O.V., Rozhdestvin V.N. *Optiko-elektronnye kvantovye pribory* (Optoelectronic Quantum Instrunments) (Moscow: Radio i Svyaz', 1982).